

## The pulsating pressure in the intake and exhaust manifold of a single cylinder engine by the various of engine revolutions

Han-Shik Chung<sup>†</sup> · Seuk-Cheun Choi\* · Hyo-Min Jong\*\* · Chi-Woo Lee\*\*\* ·  
Chi-Won Kim\*\*\*\*

(원고접수일 : 2003년 7월 18일, 심사완료일 : 2003년 11월 19일)

**Abstract** : In this research, a computer analysis has been developed for predicting the pipe pressure of the intake and exhaust manifold in a small single cylinder engine. To get the boundary conditions for a numerical analysis, one dimensional and unsteady gas dynamic calculation is performed by using the MOC(Method Of Characteristics). The main numerical parameters are engine revolutions, to calculate the pulsating flow which the intake and exhaust valves are working. The distributions of the exhaust pipe pressures were influenced strongly to the cylinder pressures, and the shapes of exhaust pressure variation were similar to the inside of cylinder pressure. As the engine revolutions are increased, the intake pressure was lower than ambient pressure. The amplitude of exhaust pressure had increased and the phase of cylinder pressure  $P_c$  is delayed and the amplitude of cylinder pressure were increased.

**Key words** : MOC(Method of Characteristics), Pressure prediction, Intake pipe, Exhaust pipe, Pulsating pressure

### Nomenclature

A : non-dimensional speed of sound { $a/a_{ref}$ }	F : cross section area of pipe[m <sup>2</sup> ]
$a_{ref}$ : reference speed of sound[m/s]	ivo : intake valve open
bdc : bottom dead center	ivc : intake valve close
D : diameter of pipe[m]	N : engine revolution[rpm]
evo : exhaust valve open	P : pressure of pipe[bar]
evc : exhaust valve close	$P_c$ : pressure of cylinder[bar]
	tdc : top dead center
	U : non-dimensional velocity{ $u/a_{ref}$ }
	u : gas velocity[m/s]

---

<sup>†</sup> 책임저자(경상대학교 기계공학부), E-mail : hschung@nongae.gsnu.ac.kr, T : 055)640-3185  
\* 해양산업연구소 특별연구원  
\*\* 경상대학교 기계항공공학부  
\*\*\* 마산대학 기계자동차공학부  
\*\*\*\* 경남대학교 기계자동차공학부

$\beta$  : Riemann variable of characteristics  
 $\lambda$  : Riemann variable of characteristics  
 $k$  : ratio of specific heats,  $[C_p/C_v]$   
 $\rho$  : density  $[\text{Kg}/\text{m}^3]$   
 $\theta$  : crank angle  $[\text{°}]$   
 $\phi$  : nozzle area ratio  $(F_t/F)$   
 cr : critical conditions  
 in : characteristic towards boundary  
 out : characteristic from boundary  
 t : throat condition

## 1. Introduction

It is very important to estimate the engine performance before a new engine development. If the development for new engine are required, the manufacturer have to change or design with competitive price and low running cost. Thus, the use of computer simulation techniques for the improvement of engine development has been rapidly expanded over the last decade. The development of CFD (Computational Fluid Dynamic) program about pressure prediction of engine manifold is need and so important. The scavenge loss by Mugele et al.<sup>(1)</sup> was simulated to a conventional two-stroke engine by applying a combination of a one dimensional and three dimensional simulation procedures. The automotive emission regulations are increased by the Environmental Protection Agency(EPA), and many of the researches for engine exhaust and manifold are reported. The pressure pulse was reported with various exhaust manifold type by using one dimensional method by Bassett et al.<sup>(2)</sup>. For the pressure prediction of small engine manifold, many numerical

calculations are utilized. Generally, the development of CFD program about pressure prediction of pipe was used by method of characteristics<sup>(3)</sup>. The method of is convenient, because the partial difference equation is converted to total difference equation by Riemann. The various boundary conditions are proposed at engine manifold suggested Benson<sup>(4-5)</sup>.

Researches about exhaust manifold of the automobile engines are increasing, but, these researches are the focused on the pressure prediction of engine cylinder for one dimensional and the unsteady compressible flow dynamics is assumed.

This research for pressure prediction in intake and exhaust manifold mainly focused on the region that the intake and exhaust valves are working. The main calculation parameters are the engine speeds with region from 3,000 rpm to 10,000 rpm.

## 2. The method of numerical solution and model

### 2.1 The method of numerical solution

The one dimensional and unsteady compressible fluid dynamics is assumed in this research. The friction and heat transfer were ignored in this research for isentropic flow. The governing equations of continuity, momentum and the characteristics of  $\lambda$ ,  $\beta$  are given as followings :

$$\frac{\partial \rho}{\partial t} + \rho \frac{\partial u}{\partial x} + u \frac{\partial \rho}{\partial x} = 0 \quad (1)$$

$$\frac{\partial u}{\partial t} + u \frac{\partial \rho}{\partial x} + \frac{1}{\rho} \cdot \frac{\partial P}{\partial x} = 0 \quad (2)$$

$$\lambda : \frac{dx}{dt} = u + a, \frac{du}{dt} = -\frac{k-1}{2} \quad (3)$$

$$\beta : \frac{dx}{dt} = u - a, \frac{du}{dt} = +\frac{k-1}{2} \quad (4)$$

2.2 Boundary condition

The length of intake and exhaust pipe is measured by real motor cycle that selected for numerical calculation model. The boundary conditions of intake and exhaust manifold for single cylinder 4-stroke engine are explained the followings, and the method of characteristics was introduced for numerical analysis.

Boundary condition of the close end,

$$\lambda_{in} = \lambda_{out} \quad (5)$$

Boundary condition of the open end,

$$\lambda_{out} = 2 - \lambda_{in} \quad (6)$$

Subsonic flow,

$$U^2 = \left(\frac{2}{K-1}\right)^2 (\lambda_{in} - A) \quad (7)$$

Sonic flow,

$$\frac{U}{A} = \phi \left(\frac{A_t}{A}\right)_{cr}^{(k+1)/(k-1)} \quad (8)$$

2.3 Numerical model

The specification of model engine as single cylinder 4-stroke engine are shown in Table 1.

Fig. 1 and Fig. 2 show the schematic diagram and photograph of motor cycle engine. The mesh generation is consisted with constant space grid, and the numbers of mesh are sixty. The

temperature and ambient pressure of numerical calculation model is 20°C and 1 bar, respectively.

Table 1 Specifications of a model engine.

engine type	4-stroke, single cylinder
engine displacement (cc)	124.1
cylinder Dia. (mm)	56.5
connecting rod length (mm)	100
stroke (mm)	49.5
intake valve open (°)	348
intake valve close (°)	568
exhaust valve open (°)	138
exhaust valve close (°)	360
compression ratio	9.5

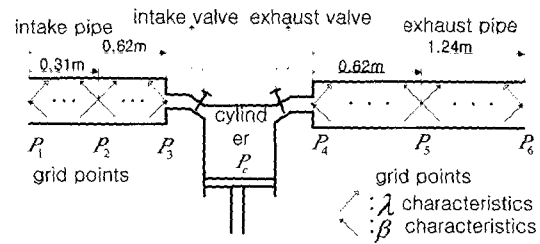


Fig. 1 Schematic diagram of numerical model for single cylinder engine

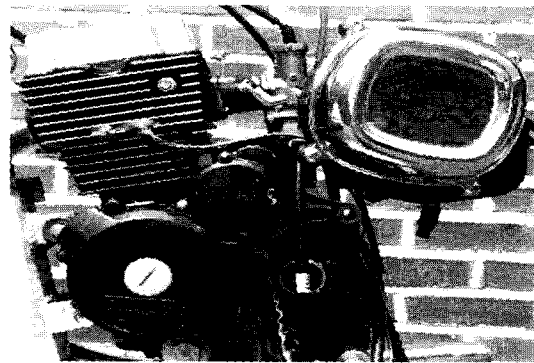
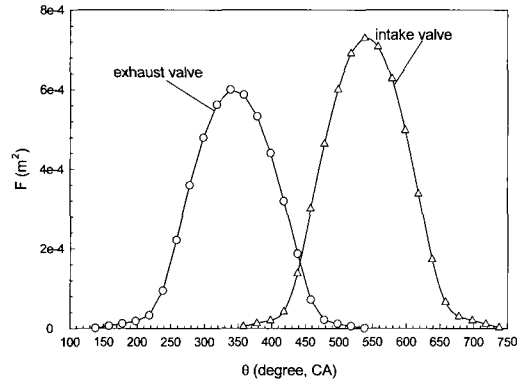


Fig. 2 Photograph of motor cycle engine

Fig. 3 shows the intake and exhaust

valve opening area according to timing. This data was obtained by measurement valve lift data. Intake valve opening timing is  $348^\circ$  and the exhaust valve opening timing is  $138^\circ$ . The intake maximum area is wider with 14 % than the exhaust maximum area.



**Fig. 3 Intake and exhaust valve opening area according to crank angle**

### 3. Results and discussions

The main numerical calculation parameters are the variation of the engine revolutions to calculate the pulsating flow during the intake and exhaust valve working.

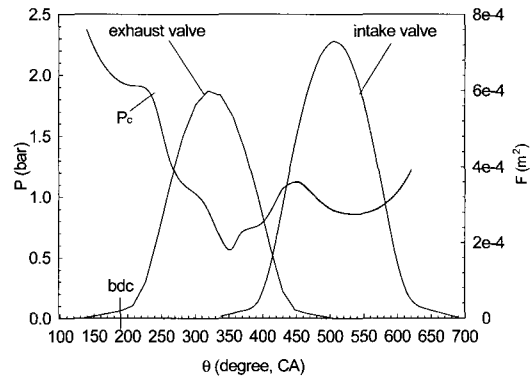
#### 3.1 Pressure distributions at engine speed 3,000 rpm

The measured intake and exhaust pipe lengths are 620 mm and 1240 mm, respectively.

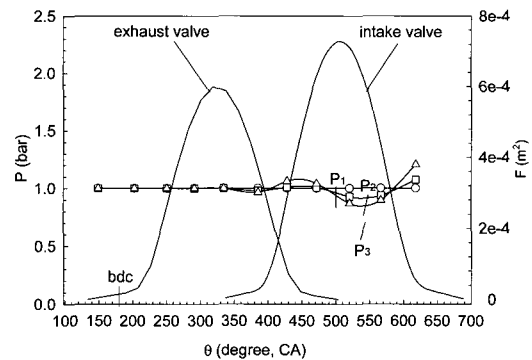
Fig. 4 shows the cylinder pressure at  $N=3,000$  rpm. The intake pipe is directly connected to the cylinder. The cylinder pressure is dropped until  $\theta=350^\circ$ . The cylinder pressure was arisen during  $\theta=350^\circ$  to  $\theta=450^\circ$ . When the cylinder

pressure has been arisen again, for instance,  $\theta=550^\circ$  and  $\theta=650^\circ$ . The reason of this pressure drop affected with intake valve open.

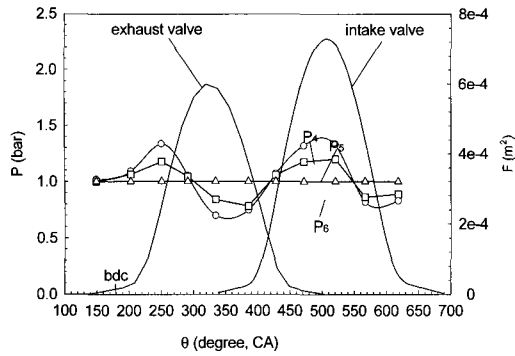
Fig. 5 shows the intake pressure variations. The pressure  $P_1$  is directly contacted to ambient, so the pressure value appears similar to ambient pressure. The pressure  $P_3$  is located near to cylinder, which controlled inlet air amount by valve lift. The minimum value of intake pressure is 0.86 bar at  $\theta=550^\circ$ . The shape of  $P_3$  in Fig. 5 after  $\theta=360^\circ$  crank angle is similar to the shape of  $P_c$  at Fig. 4.



**Fig. 4 Cylinder pressure at  $N=3,000$  rpm**



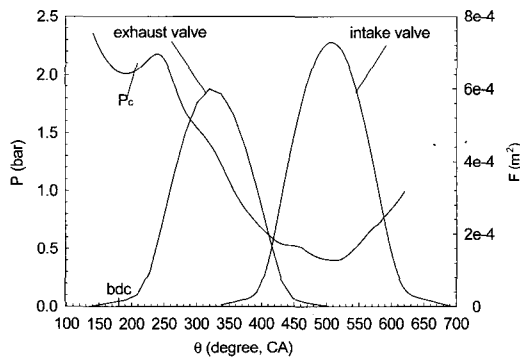
**Fig. 5 Intake pressure at  $N=3,000$  rpm**



**Fig. 6 Exhaust pressure at N=3,000 rpm**

Fig. 6 shows the exhaust pressure variation. The pressure  $P_6$  is similar to ambient pressure and have a straight line with value of 1 bar. As the pressure distribution of  $P_4$  is directly contacted with cylinder, the shape of pressure  $P_4$  is similar to the cylinder pressure after exhaust valve opening timing. When the crank angle is increased, the first peak of minimum value at pressure  $P_4$  is 1.34 bar and the peak pressure  $P_5$  is 5 % lower than the peak pressure  $P_4$ .

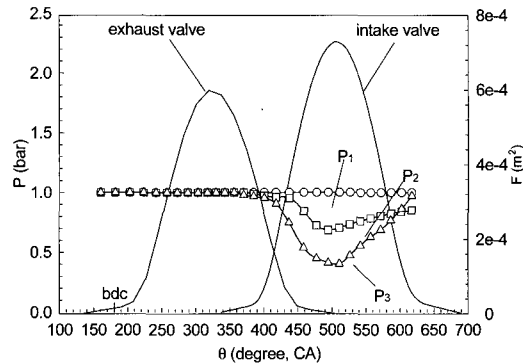
3.2 Pressure distributions at engine speed 6,000 rpm



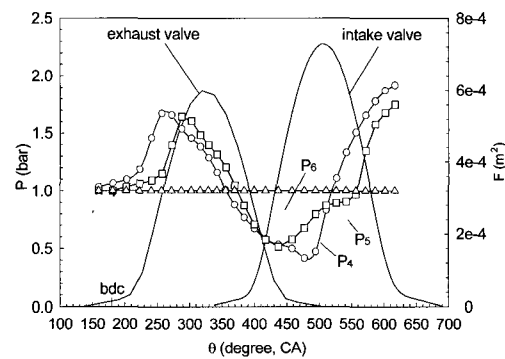
**Fig. 7 Cylinder pressure at N=6,000 rpm**

Fig. 7 shows the cylinder pressure variation at N=6,000 rpm. The cylinder

pressure has dropped under the ambient pressure until  $\theta = 520^\circ$ . The minimum cylinder pressure is 0.4 bar at  $\theta = 500^\circ$ , and the minimum value of cylinder pressure at N=6,000 rpm is 0.2bar lower than at N=3,000 rpm.



**Fig. 8 Intake pressure at N=6,000 rpm**



**Fig. 9 Exhaust pressure at N=6,000 rpm**

Fig. 8 shows the intake pressure variation at N=6,000 rpm. The shapes of intake pressure  $P_1$ ,  $P_2$  and  $P_3$  at Fig. 8 are similar to shape of cylinder pressure  $P_c$  after intake valve opening(ivo) timing. The lowest intake pressure is 0.4 bar at  $\theta = 500^\circ$ , the lowest value at N=6,000 rpm is 0.46 bar lower than N=3,000 rpm. The increasing engine revolution cause a rise of the pressure drop. The shape of intake pressure directly affected to the

shape of cylinder pressure after intake valve opening timing. The difference of pressure  $P_2$  and  $P_3$  is 0.1 bar.

Fig. 9 shows the exhaust pressure variation at  $N=6,000$  rpm. The shape of  $P_6$  is not changed, because the pressure  $P_6$  directly contacted with ambient, and that pressure value is similar to ambient pressure. The amplitude of pressure wave at the point  $P_4$  is 0.2 bar higher than one at the point  $P_4$  in Fig. 7. The first peak of maximum value is 1.69 bar at  $\theta = 270^\circ$  in the pressure  $P_4$ , which is 0.35 bar higher than the pressure  $P_4$  in Fig. 6. The peak pressure  $P_5$  is almost same value of the peak pressure  $P_4$ .

3.3 Pressure distributions at engine speed 10,000 rpm

Fig. 10 shows the cylinder pressure variation at  $N=10,000$ rpm. The cylinder pressure has dropped under the ambient pressure until  $\theta = 540^\circ$ . The shape of cylinder pressure has been changed more simplicity. The minimum cylinder pressure is 0.4 bar at  $\theta = 540^\circ$ , the minimum value of cylinder pressure at  $N=6,000$  rpm is 0.2 bar lower than one at  $N=3,000$  rpm.

Fig. 11 shows the intake pressure variation at  $N=10,000$  rpm. The shapes of intake pressure  $P_1$ ,  $P_2$  and  $P_3$  at Fig. 11 are similar to one of cylinder pressure  $P_c$  after intake valve opening(ivo) timing. The lowest intake pressure is 0.44 bar at  $\theta = 530^\circ$ , the lowest value of  $N=10,000$  rpm is 0.42 bar lower than  $N=3,000$  rpm. The higher engine speed caused the improvement of the pressure drop at both intake pipe and cylinder. The shape of

intake pressure directly affected to the shape of cylinder pressure after intake valve opening point. The difference of pressure  $P_2$  and  $P_3$  are 0.21bar. The higher engine speed caused the increasing the pressure difference between intake pressure  $P_2$  and  $P_3$ .

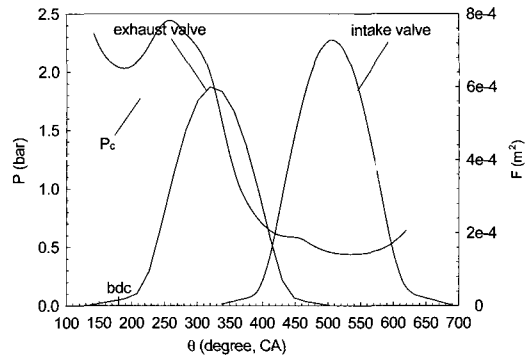


Fig. 10 Cylinder pressure at  $N=6,000$  rpm

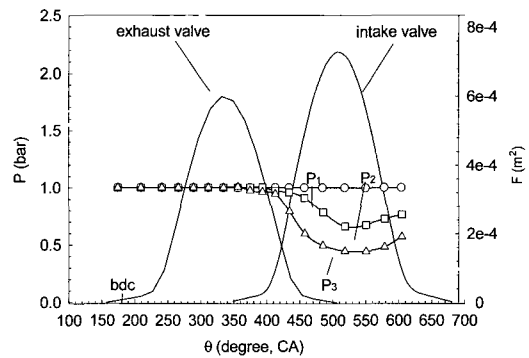


Fig. 11 Intake pressure at  $N=10,000$  rpm

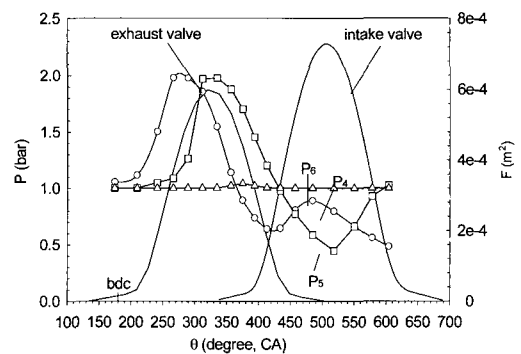
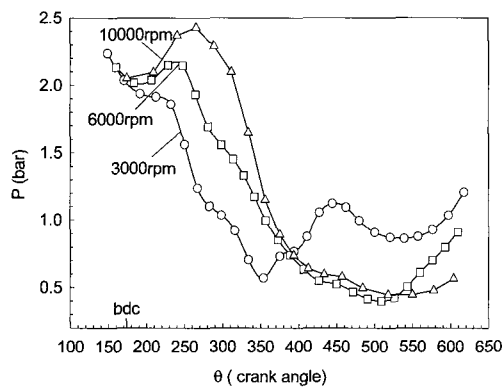


Fig. 12 Exhaust pressure at  $N=10,000$  rpm

Fig. 12 shows the exhaust pressure variation at  $N=10,000$  rpm. The shape of  $P_6$  is not changed because the pressure  $P_6$  directly contacts with ambient, that pressure value is similar to ambient pressure. The amplitude of pressure wave at the point  $P_4$  is 0.4bar higher than the point  $P_4$  in Fig. 6. The first peak of maximum value is 2.03 bar, at  $\theta=275^\circ$ , of pressure  $P_4$ , which is 0.72 bar higher than the pressure  $P_4$  in Fig. 5. Also, the wave phase was delayed about  $25^\circ$  of crank angle. Raising the engine speeds caused the increasing amplitude of exhaust pressure to increase. The peak pressure  $P_5$  is almost same value of the peak pressure  $P_4$ .



**Fig. 13 The various cylinder pressures versus crank angle.**

Fig. 13 shows the various cylinder pressure versus crank angle for the amplitude of cylinder pressure at each engine speed: 3,000 rpm, 6,000 rpm and 10,000 rpm, respectively. When the engine revolution is increasing, the amplitude has been arisen by the acceleration of piston speed near the region under the crank angle  $\theta=300^\circ$ . From the comparison between the 3,000

rpm and 6,000 rpm, the phase of the minimum cylinder pressure  $P_c$  is delayed about  $150^\circ$ . Also, the phase of the minimum cylinder pressure in case of 10,000 rpm is delayed about  $30^\circ$  in case of 6,000 rpm.

### 5. Conclusion

The results of this research about pressure prediction of intake and exhaust manifold with single cylinder 4-stroke engine are simlized as followings.

- (1) As the engine revolution is increased, the intake pressures,  $P_2$  and  $P_3$ , become lower after remaining at ambient pressure until crank angle  $\theta=400^\circ$ .
- (2) As the engine revolution is increased, the pulsating amplitude of exhaust pressure had increased.
- (3) The first peak of cylinder pressure was showed in case of 6,000 rpm at  $\theta=250^\circ$ , this peak is delayed about  $30^\circ$  in case of 10,000 rpm.
- (4) As the engine revolutions are increased, the phase of cylinder pressure  $P_c$  is delayed and the pulsating amplitude of cylinder pressure were increased.

### Acknowledgements

**This work was supported by the Brain Korea 21 Projects, Academic Research Fund and the authors gratefully appreciate the support.**

### References

[1] M.D. Bassett, D. E. Winterbone and

- R. J. Pearson, "Modelling Engines with pulse converted exhaust manifolds using one dimensional techniques" SAE Journal, vol.109 pp400-415, 2000
- [2] M. mugele, J. Tribulowski, H. Peters and U. Spicher., "Numerical analysis of gas exchange and combustion process in a small two stroke gasoline engine" SAE Journal, Vol. 110, no. 3, pp29-35, 2001
- [3] R. S. Benson., 1982, The Thermodynamics and Gas Dynamics of Internal-Combustion Engines, Clarendon Press Vol.1, pp246-325
- [4] E. D. Winterbone., and Pearson, J. R., "Theory of Engine Manifold Design" Professional Engineering Publishing Limited, pp18-46, 2000
- [5] M. badami, F. millo and G. Giaffreda, "Experimental and Computational Anylisis of a High Performance Four stroke Motorcycle Engine Equipped with a Variable Geometry Exhaust System" SAE proceeding paper 2002-01-0001
- [6] D. O. Mackey, J. G. Crandall, G. F. Chatfield and M. C. Ashe "Optimization of Exhaust-Pipe Tuning on a 4-stroke Engine Using Simulation" SAE proceeding paper 2002-01-0002

## 저 자 소 개



### 최석천 (崔碩天)

1972년 10월생, 2000년 경상대학교 선박기계공학과 졸업, 2003년-현재 경상대학교 정밀기계 대학원 석사수료, 현재 해양산업연구소 특별연구원



### 정한식 (鄭漢植)

1954년 4월생, 1981년 동아대학교 기계공학과 졸업, 1987년 동 대학원 기계공학과 박사학위, 1981년-1985년 대림자동차공업(주) 기술부, 1988년-1991년 창원기능대학 열설비학과, 1995년-2003년 현 경상대학교 기계항공공학부 부교수



### 정효민 (鄭孝玟)

1958년 12월생, 1978년-1982년 부경대학교 공학사, 1984년-1987년 부경대학교 공학석사, 1988년-1992년 Univ. of Tokyo, Japan 공학 박사, 1995년-1999년 경상대학교 조교수, 1999년-2000년 Univ. of Central Florida (Florida Solar Energy Center), Visiting Professor, 1999년 10월-현재 경상대학교 기계항공공학부 부교수



### 이치우 (李致雨)

1965년 8월생, 1991년 동아대학교 기계공학과 졸업, 1993년 동대학원 기계공학과 졸업(석사), 2000년 동대학원 기계공학과 졸업(공학박사), 1995~현재 마산대학 기계자동차공학부 교수, 당학회 회원